ARTICLES

Ground- and Excited-State Isomerization of Triphenylmethane Dyes in the Femtosecond Regime

Yoshihiro Maruyama,*,†,⊥ Olivier Magnin,‡ Hiroshi Satozono,§ and Mitsuru Ishikawa*,†,⊥

Hamamatsu Photonics K. K.,Tsukuba Research Laboratory, 5-9-2 Tokodai, Tsukuba, Ibaraki 300-2635, Japan

Received: November 10, 1998; In Final Form: February 22, 1999

We previously confirmed the existence of two ground-state isomers of crystal violet (CV) in alcohol (Maruyama, Y.; Ishikawa, M.; Satozono, H. *J. Am. Chem. Soc.* **1996**, *118*, 6257). These isomers are called "solvation isomers" because they are differentiated by the solvation of alcohol. Here, to investigate if solvation isomers are possible in triphenylmethane (TPM) dyes other than CV, we measured transient differential absorption (ΔOD) spectra of two classes of TPM dyes: symmetric (ethyl violet and parafuchsin) and asymmetric (malachite green and brilliant green) using a femtosecond spectral hole-burning technique. The symmetric TPM dyes that we studied (including CV) showed two spectral holes in the early part of photobleaching, whereas the asymmetric dyes showed three spectral holes. The ΔOD spectra of all of the TPM dyes depended on the pump wavelength. This dependence is the key experimental observation that confirms the existence of ground-state isomers, and thus the asymmetric TPM dyes have three ground-state isomers. Solvation isomers are possible in TPM dyes in alcohol. To obtain insight into the deactivation mechanism of TPM dyes, we examined a plateau region that appears in the early part of photobleaching recovery. The plateau is evidence for the existence of an intermediate state between the lowest singlet excited state (S_1) and the ground state. The absence of the plateau only in parafuchsin, which is due to the difference in a positive charge distribution on a nitrogen atom, suggests that the intermediate state is a distorted excited state in which a positive charge is partially shifted to a nitrogen atom in an amino group.

Introduction

Triphenylmethane (TPM) dyes have long been studied for their molecular structures,[1−3] electronic states,[4−9] and relaxation dynamics.[10−17] The relaxation time of the excited state of TPM dyes is much faster (on the order of picoseconds) in low-viscosity solvents such as methanol,[11,12,18−20] compared with the relaxation time of typical fluorescent dyes (nanoseconds), such as nile blue and rhodamine B. Based on the molecular structure and on the solvent viscosity dependence of the fluorescence lifetimes[10,12,20,21,22−24] of TPM dyes, this ultrafast relaxation is believed to be due to nonradiative relaxation induced by rotation or torsion of the phenyl rings. The existence of ground-state isomers of crystal violet (CV), which is a TPM dye, has long been disputed.[8,20,25−27] By using the femtosecond spectral hole-burning technique, we recently confirmed that CV in alcohol has two ground-state isomers.[18,19] The early part of the transient differential absorption (ΔOD) spectra of CV in alcohol showed two spectral holes, at 550 and 600 nm. The growth of these holes depended on the pump wavelength and on the probe wavelength. When the pump wavelength was 548 nm, both of the spectral holes appeared simultaneously, whereas when the pump wavelength was 598 nm, the appearance of the hole at 550 nm lagged behind that of the hole at 600 nm. These observations show that the ground state of CV in alcohol is inhomogeneous; that is, two isomers are present. Moreover, as the experimental temperature was decreased, the absorption peak at 550 nm decreased, whereas the absorption peak at 600 nm increased. This temperature dependence of the absorption spectra further confirms the existence of the ground-state isomers.[25] To identify the structure of these isomers, in our previous study we used molecular orbital calculations to study the effects of a solvent molecule on the molecular structure of CV. On the basis of the results, we proposed a model of the isomers that accounts for the difference in the solvation of alcohol: one is planar and the other is pyramidal, which we termed "solvation isomers" as a novel class of isomers.[19]

Our current study had two goals involving the ground- and excited-state isomerization of TPM dyes. The first goal was to determine if solvation isomers in the ground state are common to TPM dyes other than CV. TPM dyes are classified according to their structure: (i) asymmetrical, where one of the phenyl rings has no functional groups; and (ii) symmetrical, where all

* To whom correspondence should be addressed. Phone: +81-298-47-5161. Fax: +81-47-5266. E-mail: maruyama@hpk.trc-net.co.jp.

† Hamamatsu Photonics K. K., Tsukuba Research Laboratory.

‡ Laboratoire des Systèmes Photoniques, Ecole Nationale Supèrieur de Physique de Strasbourg, Boulevard Sèbastien Brandt, 67400 Illkirch, France. Present address: ABX Haematology, Parc Euromedecine, Rue du Caducee, 34184 Montpelier, France.

§ Hamamatsu Photonics K. K., Central Research Laboratory, eighth Research Group, Hamakita Research Park, 5000 Hirakuchi, Hamakita, Shizuoka 434-0041, Japan.

⊥ Present address: JRCAT-ATP, 1-1-4 Higashi, Tsukuba, Ibaraki 305-0046, Japan.

10.1021/jp984376z CCC: $18.00
Published on Web 07/02/1999

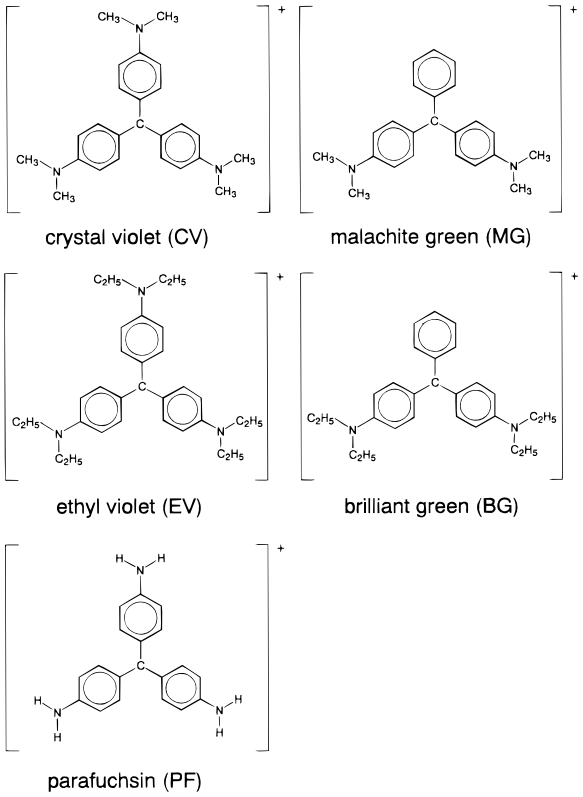

Figure 1. Molecular structures of the TPM dyes used in this study.

of the phenyl rings have the same kind of functional group. We studied two asymmetrical dyes (Figure 1), malachite green (MG) and brilliant green (BG), and two symmetrical dyes, ethyl violet (EV) and parafuchsin (PF). Using the femtosecond spectral hole-burning technique, we found evidence for two ground states in the symmetry group and for three ground states in the asymmetry group. We also estimated the isomerization rate in the ground state by analyzing the temporal profile of the ΔOD spectra of the TPM dyes.

The second goal was to examine the substitution effect on the deactivation behavior to further understand the deactivation mechanism. Except for PF, all of the TPM dyes studied here showed a "plateau" region in the early part of the bleaching recovery (Figure 7), evidence of a time lag in the bleaching recovery.[11,13−15,28] The plateau shows the existence of an intermediate state between the S_1 state and the ground state. A distorted excited state isomer was previously proposed as an origin of the intermediate state.[13−15] Here, we obtained more convincing evidence that the intermediate state is the distorted excited state. Among the TPM dyes that we studied, only PF lacked the plateau of the bleaching recovery, showing that a positive charge is partially shifted to a nitrogen atom in an amino group in the intermediate state. We evaluated the rate of this positive charge transfer by determining the isomerization rate in the excited state.

Experimental Section

We observed the temporal profile of the ΔOD spectra of the TPM dyes using the femtosecond spectral hole-burning technique. We used methanol solutions of the TPM dyes as samples. All dyes were purchased from Nakalai-Tesque (Kyoto, Japan), GR grade, and used without further purification. The solvent was spectrosol grade methanol supplied by Dojin (Tokyo, Japan). At a concentration of 5×10^{-4} M, the dyes did not aggregate in the prepared solutions. The dye solution was circulated to avoid thermal decomposition, and passed through a 0.5 mm thick quartz cell, where the pump and probe pulses mutually crossed.

The spectral hole-burning experiments were done at room temperature (295 K). The details of the femtosecond dye laser system and the femtosecond pump−probe spectrometer are described elsewhere.[18,19] The full width at the half-maximum (fwhm) of the pump and probe pulses were ∼400 and ∼200 fs, respectively. The pump-pulse energy was ∼100 μJ/pulse and the diameter of the pump pulse on the sample was ∼2 mm. Polarization of the pump pulse and that of the probe pulse were mutually parallel (p-polarization). The time scale of rotational diffusion of TPM dyes is slow with respect to that of the ground-state recovery in methanol.[29] The pump wavelength was 550, 560, 600, or 640 nm, all of which were selected with interference filters (5 or 10 nm fwhm). The probe light was white light continuum centered at ∼600 nm. The time interval of the ΔOD spectra was 200 fs. All ΔOD spectra were corrected for the group delay of the probe pulses.

We also estimated the charge distribution of CV, EV, and PF in the ground state by calculating the molecular orbital using the MNDO-PM3 method (modified neglect of diatomic overlap, parametric method 3)[30] with the program MOPAC Version 6. The three steps in the calculation were (1) calculating the charge distribution of the free dyes, (2) calculating the equilibrium distance between a dye molecule and a methanol molecule, and (3) calculating the charge distribution of the complex between a dye molecule and a methanol molecule. In the complex the methanol molecule is at the equilibrium location on a nitrogen atom of the dye.

Results

ΔOD Spectra of the Asymmetric TPM Dyes, MG and BG. The ΔOD spectra of MG and BG in methanol were similar in shape and temporal profile. We therefore only discuss the results for BG. In the growth of the ΔOD spectra of BG in methanol (Figure 2), transient absorption from S_1 to S_n occurred in the region where the wavelength was shorter than the ground-state absorption maxima (<550 nm), whereas stimulated emission gain occurred where the wavelength was longer than the ground state absorption maxima (>670 nm). For all pump wavelengths studied here, each spectrum showed three spectral holes (570, 620, and 635 nm). However, the growth of each hole depended on the pump wavelength. Figure 3 shows the temporal profiles of ΔOD at the probe wavelengths that correspond to each of the spectral holes. When the pump wavelength was 560 nm, the three holes appeared simultaneously. When the pump wavelength was 600 nm, the holes at 618 and 645 nm appeared simultaneously, whereas the hole at 584 nm appeared after a time delay. When the pump wavelength was 640 nm, the holes appeared separately: the hole at 645 nm appeared first, then the hole at 618 nm, and finally the hole at 584 nm. The bleaching recovery curves of MG and BG both had a plateau, which is evidence of an intermediate state between S_1 state and S_0 state.[11,13−15,28]

We curve-fitted the temporal profile of the growth and recovery of the bleaching using the following convolution

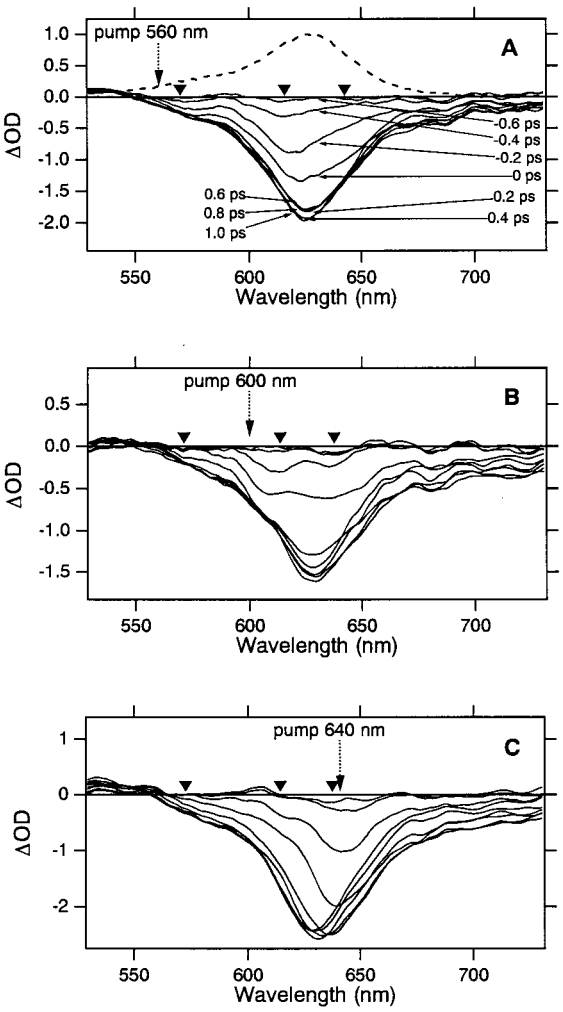

Figure 2. ΔOD spectra of BG in methanol at 295 K for a pump wavelength of (A) 560 nm, (B) 600 nm, and (C) 640 nm. The probe delay was from −0.6 to 1.0 ps at an interval of 200 fs. The dashed line in the upper record in (A) shows the ground-state absorption spectrum of BG, the arrows with dotted lines show the pump-pulse wavelengths, and the triangles show the positions of the bleaching bands.

formula:

$$I(t) = \int_{-\infty}^{t} p(t')\,[1 - \exp(-(t-t')/\tau_r)]\sum_i A_i\left[\frac{1}{\tau_i}\exp(-(t-t')/\tau_x) - \frac{1}{\tau_x}\exp(-(t-t')/\tau_i)\right]\mathrm{d}t' \quad (1)$$

where $I(t)$ is the degree of ΔOD at time t and $p(t')$ is the intensity of the pump pulse at time t'. We used the following fitting parameters: A_i is a coefficient, τ_r is the time delay of the growth of the bleaching, τ_x is the transition time from the excited state (just after excitation) to the intermediate state, and τ_i ($i = 1, 2$) is the relaxation time from the intermediate state to the ground state. First, we obtained τ_i from fitting of the data measured in long time range (−3 to 100 ps). Second, the other parameters were obtained from fitting of the data measured in short time range (−3 to 8 ps). The fitting parameters for BG in methanol (Table 1) show that τ_r depended on the pump and probe wavelengths, whereas τ_i was independent of those wavelengths. The ground-state recovery time τ_i had faster and slower components.

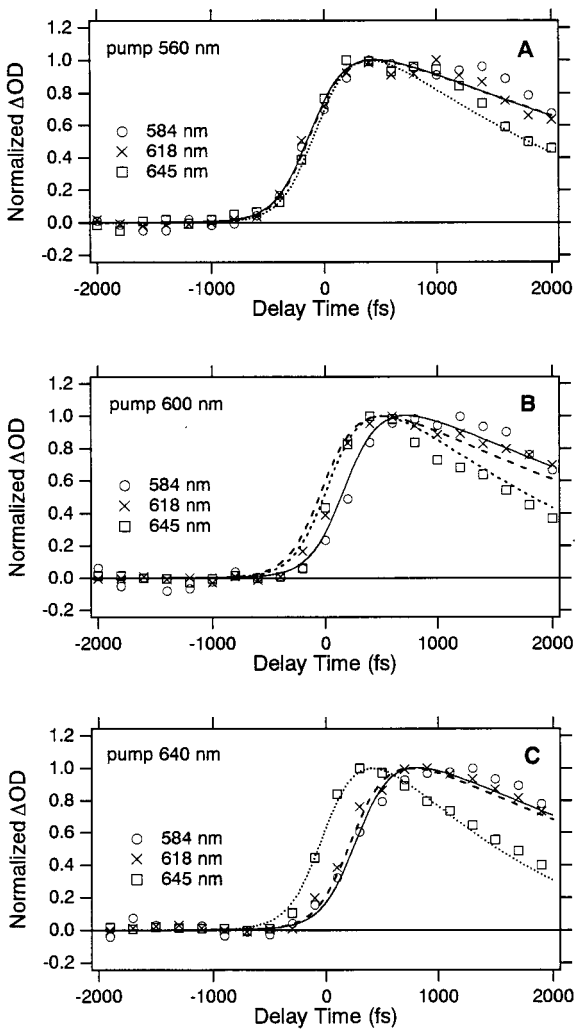

Figure 3. Time evolution of the photobleaching of BG in methanol at 295 K. The pump wavelengths are (A) 560 nm, (B) 600 nm, and (C) 640 nm. The best fit functions are along with the data proved at 584 nm (solid line), 618 nm (broken line), and 645 nm (dotted line).

TABLE 1: Fitting Parameters for the Bleaching Recovery Curves of BG in Methanol

probe (nm)	pump 560 nm τ_r[a]	τ_x[a]	τ_i[a]	600 nm τ_r[a]	τ_x[a]	τ_i[a]	640 nm τ_r[a]	τ_x[a]	τ_i[a]
584	0	1000	1300	200	1200	1300	700	1000	1050
618	0	1000	1100	0	1000	1500	400	1100	1150
		1000	6500		1000	6500		1050	6500
645	0	1000	1100	50	900	1000	0	500	1200
		1000	6500		1000	6500	0	500	6500

[a] In femtoseconds.

ΔOD Spectra of the Symmetric TPM Dyes, EV and PF. In the growth of the ΔOD spectra of EV in methanol (Figure 4), the shape was similar to that of CV.[18,19] Transient absorption from S_1 to S_n occurred where the wavelength was shorter than the ground-state absorption maxima (<500 nm). Stimulated emission gain occurred where the wavelength was longer than the ground-state absorption maxima (>620 nm). Two spectral holes (at 550 and 600 nm) appeared in the ΔOD spectra of EV. The growth of the spectral holes depended on the pump wavelength and probe wavelength. The temporal profile of the two spectral holes in the ΔOD spectra of EV in methanol (Figure 5) shows that when the pump wavelength was 560 nm, both of the holes appeared simultaneously, whereas when the pump

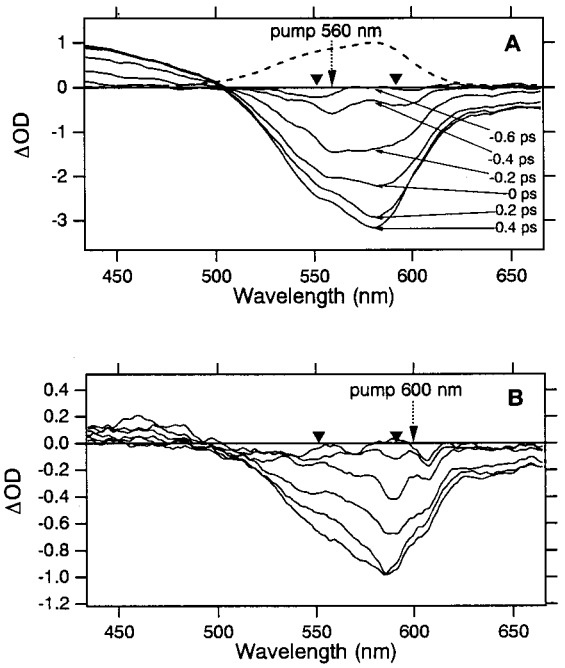

Figure 4. ΔOD spectra of EV in methanol at 295 K for a pump wavelength of (A) 560 nm and (B) 600 nm. The probe delay was from −0.6 to 0.4 ps at an interval of 200 fs. The dashed line in the upper record in (A) shows the ground-state absorption spectrum of EV, the arrow with the dotted line shows the pump wavelength, and the triangles show the positions of the bleaching bands.

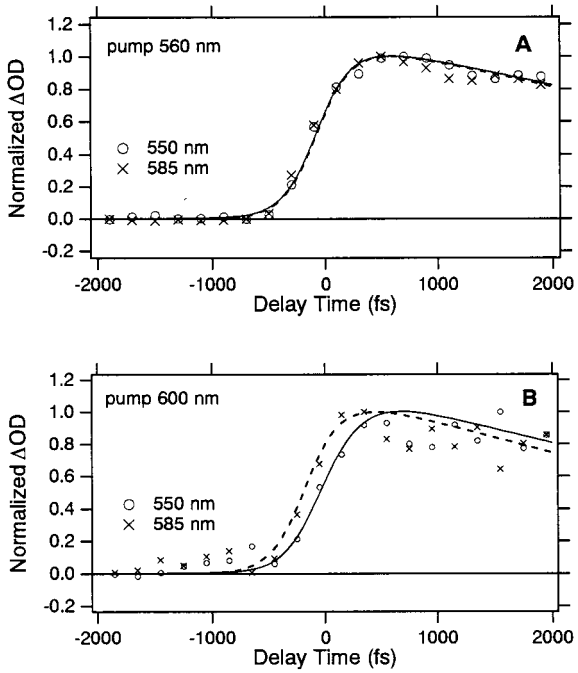

Figure 5. Time evolution of the photobleaching of EV in methanol at 295 K. The pump wavelengths are (A) 560 nm and (B) 600 nm. The best fit functions are along with the data proved at 550 nm (solid line) and at 585 nm (broken line).

wavelength was 600 nm, first the hole at 600 nm appeared and then the hole at 550 nm appeared. The bleaching recovery curve of EV in methanol showed a plateau. The ΔOD spectra of PF in methanol were similar in shape to those of CV and EV in methanol except for spectrally shifting to shorter wavelength (Figure 6A). The ΔOD spectra of PF showed two holes, at 510 and 550 nm. The temporal profiles of these two spectral holes (Figure 6B) show that when the pump wavelength was near

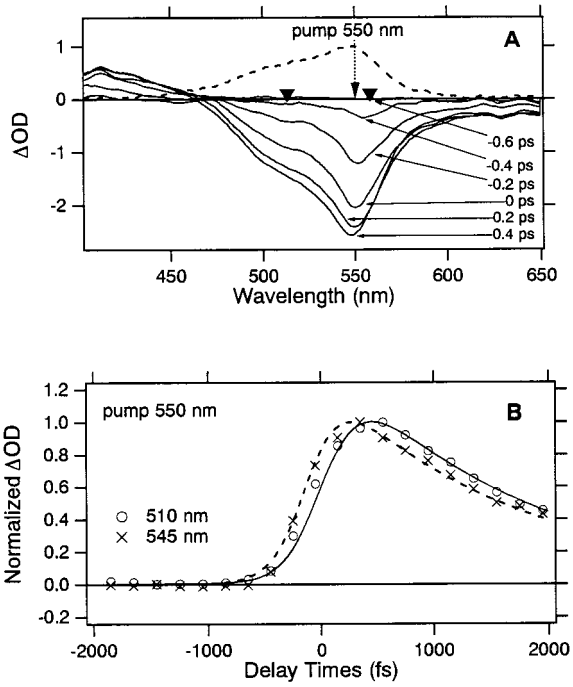

Figure 6. (A) ΔOD spectra of PF in methanol at 295 K and (B) the time evolution of the spectral bleaching of PF in methanol for a pump wavelength of 550 nm. The probe delay was from −0.6 to 0.4 ps at an interval of 200 fs. The dashed line in the upper record in (A) shows the ground-state absorption spectrum of PF, the arrow with the dotted line shows the pump wavelength, and the triangles show the positions of the bleaching bands. The best fit functions are along with the data proved at 510 nm (solid line) and at 545 nm (broken line) in (B).

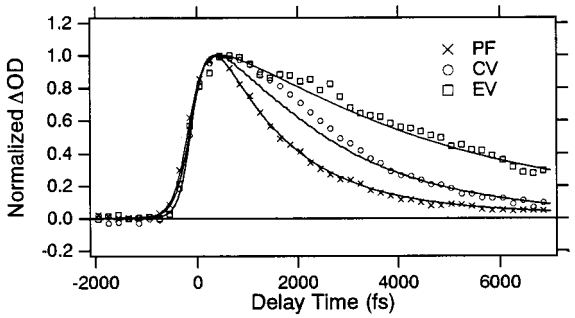

Figure 7. Time evolution of the spectral bleaching of PF, CV, and EV in methanol at 295 K for a probe wavelength of 510 nm for PF, and 550 nm for CV and EV. The best fit functions are along with the data.

the absorption maximum (550 nm), the spectral hole at 510 nm appeared after the hole at 550 nm. For PF we were unable to use a pump wavelength shorter than 550 nm, because available wavelengths were limited by the femtosecond amplifier in which a frequency doubled (532 nm) Nd:YAG laser was used. Figure 7 shows the temporal profiles of the ΔOD of PF, CV, and EV in methanol. Each of the probe wavelengths corresponds to the shorter wavelength hole in the ΔOD spectra of each dye. The bleaching recovery curve of PF showed no plateau. We used eq 1 to curve fit the ΔOD of EV and PF. The results (Table 2) show that as the size of the functional group connected with the phenyl ring was increased, the faster component of the bleaching recovery time (τ_i) increased (1.5 to 3.0 or 3.5 ps). More importantly, the estimated transition time from the excited state to the intermediate state (τ_x) of PF in methanol was ∼0 fs, whereas that for CV and EV was ∼1000 fs.

The molecular orbital calculations of the charge distribution on a nitrogen atom in PF, CV, and EV (Table 3) show that as

TABLE 2: Fitting Parameters for the Bleaching Recovery Curves of EV and PF in Methanol

EV							PF			
	pump							pump		
probe	560 nm			600 nm			probe	550 nm		
(nm)	τ_r[a]	τ_x[a]	τ_i[a]	τ_r[a]	τ_x[a]	τ_i[a]	(nm)	τ_r	τ_x	τ_i
550	0	1000	3500	150	1000	3000	510	150	0	1500
		1000	6500		1000	6500			0	6500
585	0	1000	3500	0	1000	3000	545	0	0	1500
		1000	6500		1000	6500			0	4000

[a] In femtoseconds.

TABLE 3: Molecular Orbital Calculation of Charge Distribution on a Nitrogen (N) Atom of Selected TPM Dyes in the Ground State

	free	interacting with a methanol molecule	
dye	positive charge on a N atom (e)	positive charge on a N atom (e)	distance (Å)[a]
PF	+0.1599	+0.1726	3.06
CV	+0.0916	+0.1147	3.68
EV	+0.0792	+0.0558	3.88

[a] Distance between a nitrogen atom of the dye and an oxygen atom of the methanol.

the size of the functional group connected with a phenyl ring increased, the positive charge on a nitrogen atom decreased. Except for EV, when a methanol molecule was located at a nitrogen atom, the positive charge on the nitrogen atom was larger than that without a methanol molecule.

Discussion

Ground-State Isomers of TPM Dyes. Three spectral holes appeared in the ΔOD spectra of MG and BG in methanol, and their growth depended on the pump wavelength. This appearance and pump-wavelength dependence of multiple holes means that the ground states of MG and BG in methanol are inhomogeneous. The inhomogeneity of the ground state based on ΔOD spectra was previously discussed in depth for CV.[18,19] The key point from that discussion is that if the ground state is homogeneous, then the temporal rise in ΔOD spectra should be independent of pump wavelength. If the observations were due to the inhomogeneous broadening of vibrational bands, that is, the direct burning of the hole close to the excitation wavelength and the broadening of the initial hole, when pumped at shorter side of the absorption spectrum, the hole close to the pump wavelength should show fast rise. However, all holes were appeared simultaneously when pumped at the shorter side of the absorption spectrum. In addition, with the same experimental setup we did similar spectral hole-burning experiment for nile blue and cresyl violet in methanol, both of which are more rigid molecules than TPM dyes. There was no pump wavelength dependence in their transient ΔOD spectra. The growth of the spectral holes in the ΔOD spectra of MG and BG can be explained with an energy diagram showing three ground states (Figure 8), where each ground state (S_0) corresponds to isomers and each isomer to H, M, and L in the order of absorption maxima. The temporal rise of the bleaching of BG in methanol is explained as follows. When the pump wavelength is 560 nm, all isomers are excited, and the transitions from the ground state to the excited state of all isomers are saturated simultaneously. When the pump wavelength is 600 nm, isomers M and L are excited, and the absorption of both M and L is saturated. If the potential barriers from H to M or from H to L are comparable

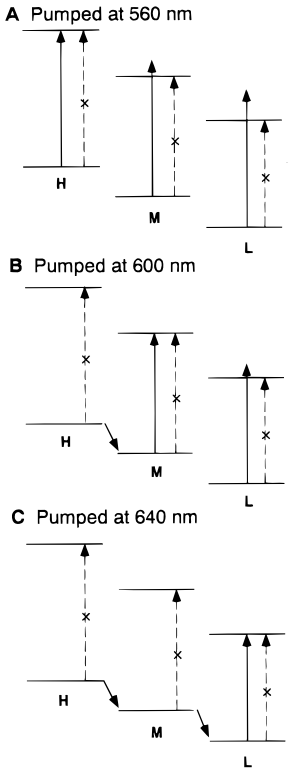

Figure 8. Energy level scheme of MG and BG in methanol. The arrows with solid lines represent electronic transitions by pump light or the population transfer from the higher ground state to the lower ground state. The arrows with the dotted lines are electronic transitions by the probe light. The symbol × means that the transition is saturated.

to the thermal energy at the experimental temperature (295 K), then the isomerization from H to M or from H to L approach thermal equilibrium at a rate related to the height of the potential barrier. This isomerization causes a decrease in the population of H, thus causing a time delay in the bleaching of the ground state absorption of H. When the pump wavelength is 640 nm, only isomer L is excited. Similar to what happens at a pump wavelength of 600 nm, the decrease in the population of L causes thermal nonequilibrium. To reach thermal equilibrium, isomerization from H and M to L occurs, thus resulting in a time delay of the bleaching of the absorption of H and M. Therefore, the rise time τ_r in Table 1 is the isomerization rate in the ground states.

For CV in methanol, we previously proposed solvation isomers as a model of the ground-state isomers.[19] Although our results here do not provide details of a molecular structure model of the three ground states of MG and BG, solvation isomers may also be applicable in the ground states of MG and BG in methanol. The reason is that the pump-wavelength dependence of the temporal rise in the bleaching recovery of MG and BG in methanol was similar to that of CV, although MG and BG showed three spectral holes whereas CV showed two spectral holes.

The pump- and probe-wavelength dependence of the bleaching spectra of EV and PF was similar to that of CV.[18,19] This dependence is explained by a potential energy diagram that includes two ground-state isomers, similar to CV in methanol. Solvation isomers may also be applicable in EV and PF in methanol. The rise time τ_r in Table 2 is the isomerization rate in the ground states. The isomerization in the ground state of the TPM dyes in methanol occurs in the femtosecond regime.

Origin of the Intermediate State. The estimated transition rate τ_x from the excited state to the intermediate state was ≈0

fs for PF, confirmed by the absence of a plateau in the bleaching recovery curve. The intermediate state of CV, EV, and MG has already been discussed, and three possibilities for the intermediate state have been proposed: (i) hot ground state,[11] (ii) twisted intramolecular charge transfer state (TICT) in the excited state,[16] and (iii) distorted excited-state isomer without clear charge separation, unlike TICT.[13−15] Martin et al. observed the ΔOD spectra of EV in several solvents, such as ethanol, dioxane, tetrahydrofuran, and decanol, and obtained the absorption spectrum of the intermediate state.[14] The rates of formation and deactivation of the intermediate state are similar to each other in ethanol and in dioxane. The viscosity of ethanol (1.08 cP) is similar to that of dioxane (1.09 cP), whereas the dielectric constant of ethanol (24.5) is about 10 times higher than that of dioxane (2.2). Martin et al. therefore excluded the TICT model as the intermediate state because the TICT state should be sensitive to the dielectric constant of the solvents. Moreover, the intermediate state absorption persisted more than 70 ps in viscous alcohols such as decanol. This persistence shows that the intermediate state is not the hot ground state, because such slow solute−solvent energy transfer occurs only for solvents that do not contain C−H bonds (e.g., CCl_4).[31] Martin et al. concluded that the intermediate state is a distorted excited state, and that the absorption spectrum of the intermediate state is similar to that of S_1 but spectrally shifted to a higher energy level. This similarity supports the distorted excited state model. However, the intermediate state possibly has a charge-transfer nature, because molecular distortion and subunit rotation are concomitant with the change in the charge distribution. The Bagchi−Fleming−Oxtoby (BFO) model of barrierless isomerization in the excited state can also explain that the plateau region in the ground-state recovery is due to the excited-state isomerization.[32] The observed nonexponential ground-state recovery, which contains faster and slower time constant, can be explained with the BFO model.

Our study also supports the distorted excited-state model as the intermediate state. The plateau of the bleaching recovery curve, confirming the existence of the intermediate state, was not observed in the decay curve of the bleaching of PF. This absence means that the transition rate from the excited state (just after excitation) to the intermediate state is much faster in PF than in CV and EV. Because the difference between CV and PF is that the functional group connected with each phenyl ring is a dimethylamino group for CV and an amino group for PV, the intermediate state must be related to this functional group. This difference in functional group causes the difference in the charge distribution among the dyes. The calculated charge distribution at the ground state of the dyes (Table 3) shows that the positive charge was more localized at a nitrogen atom in PF than that in CV and EV. Assuming that the intermediate state is the distorted excited state with a positive charge localized on a nitrogen atom, the excited state just after excitation for PF has already more similar charge distribution to the intermediate state than for CV and EV. Thus, the transition to the intermediate state would be faster for PF than for CV and EV. Figure 9 shows a schematic of the excitation and relaxation dynamics of CV, EV, MG, BG, and PF. The excited-state isomerization rate, $k_x = 1/\tau_x$, was $\sim 1 \times 10^{12}$ s^{-1} for CV, EV, MG, and BG in methanol. The isomerization in the excited-state of the TPM dyes occurs in the femtosecond regime. The reaction coordinate is along the charge transition from the central carbon atom to the nitrogen atom. This reaction involves changes in the charge distribution and molecular structure. For clarity in Figure 9, we show the charge distribution in the structural formulas as a positive charge of unity rather than an actual partial positive charge.

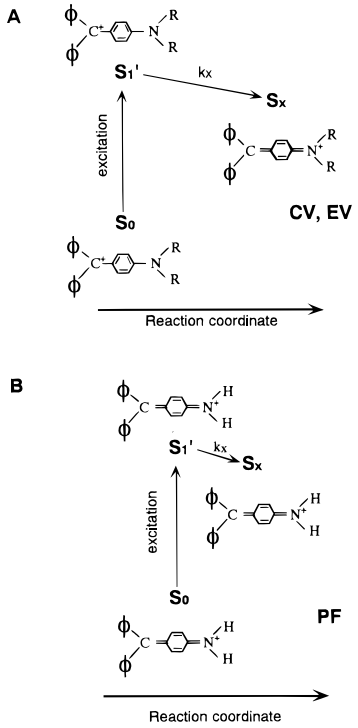

Figure 9. Scheme of the transition dynamics from the ground state to the intermediate state of (A) CV and EV and (B) PF in methanol. S_1' is the Franck−Condon state, S_x is the intermediate state, and the transition rate k_x is $1/\tau_x$. The reaction coordinate is along the positive charge transition from the central carbon atom to the nitrogen atom. In the structural formulas, ϕ is dimethylaminophenyl group for CV, diethylaminophenyl group for EV, and aminophenyl group for PF. R is methyl group for CV, and ethyl group for EV.

Conclusion

Using a femtosecond spectral hole-burning technique, we confirmed that the ground state of TPM dyes in methanol is inhomogeneous. We used ground- and excited-state isomerization to explain the time evolution of the ΔOD spectra. The ΔOD spectra of all of the TPM dyes studied here depended on the pump wavelength. This dependence is due to the existence of two or three ground-state isomers and to the isomerization between them, as previously proposed for CV. The concept of solvation isomer is therefore applicable to TPM dyes in alcohol. Our results show that substitution of a functional group connected with a phenyl ring in symmetrical TPM dyes affects the plateau feature in the temporal profile of bleaching recovery. The absence of this plateau only in PF is evidence that the intermediate state in the deactivation process of the excited state is a distorted excited-state isomer involving positive charge transfer to a nitrogen atom. Thus, the origin of the plateau is the excited-state isomerization.

References and Notes

(1) Gomes de Mesquita, A. H.; MacGillavry, C. H.; Eriks, K. *Acta Crystallogr.* **1965**, *18*, 437.
(2) Dekkers, H. P. J. M.; Kielman-Van Luyt, E. C. M. *Mol. Phys.* **1976**, *31*, 1001.
(3) Angeloni, L.; Smulevich, G.; Marzocchi, M. P. *J. Raman Spectrosc.* **1979**, *8*, 305.
(4) Looney, C. W.; Simpson, W. T. *J. Am. Chem. Soc.* **1954**, *76*, 6293.
(5) Adam, F. C.; Simpson, W. T. *J. Mol. Spectrosc.* **1959**, *3*, 363.
(6) Korppi-Tommola, J.; Yip, R. W. *Can. J. Chem.* **1981**, *59*, 191.

(7) Korppi-Tommola, J.; Kolehmainen, E.; Salo, E.; Yip, R. W. *Chem. Phys. Lett.* **1984**, *104*, 373.
(8) Lueck, H. B.; McHale, J. L.; Edwards, W. D. *J. Am. Chem. Soc.* **1992**, *114*, 2342.
(9) Duxbury, D. F. *Chem. Rev.* **1993**, *93*, 381.
(10) Cremers, D. A.; Windsor, M. W. *Chem. Phys. Lett.* **1980**, *71*, 27.
(11) Ben-Amotz, D.; Harris, C. B. *Chem. Phys. Lett.* **1985**, *119*, 305.
(12) Ben-Amotz, D.; Harris, C. B. *J. Chem. Phys.* **1987**, *86*, 4856.
(13) Martin, M. M.; Breheret, E.; Nesa, F.; Meyer, Y. H. *Chem. Phys.* **1989**, *130*, 279.
(14) Martin, M. M.; Plaza, P.; Meyer, Y. H. *Chem. Phys.* **1991**, *153*, 297.
(15) Martin, M. M.; Plaza, P.; Meyer, Y. H. *J. Phys. Chem.* **1991**, *95*, 9310.
(16) Vogel, M.; Rettig, W. *Ber. Bunsen-Ges. Phys. Chem.* **1985**, *89*, 962.
(17) Vogel, M.; Rettig, W. *Ber. Bunsen-Ges. Phys. Chem.* **1987**, *91*, 1241.
(18) Ishikawa, M.; Maruyama, Y. *Chem. Phys. Lett.* **1994**, *219*, 416.
(19) Maruyama, Y.; Ishikawa, M.; Satozono, H. *J. Am. Chem. Soc.* **1996**, *118*, 6257.
(20) Sundström, V.; Gillbro, T. J. *Chem. Phys.* **1984**, *81*, 3463.
(21) Förster, T.; Hoffmann, G. Z. *Phys. Chem. NF* **1971**, *75*, 63.
(22) Ye, J. Y.; Hattori, T.; Inouye, H.; Ueta, H.; Nakatsuka, H.; Maruyama, Y.; Ishikawa, M. *Phys. Rev.* **1996**, *B 53*, 8349.
(23) Ye, J. Y.; Hattori, T.; Nakatsuka, H.; Maruyama, Y.; Ishikawa, M. *Phys. Rev.* **1997**, *B 56*, 5286.
(24) Ye, J. Y.; Ishikawa, M.; Yogi, O.; Okada, T.; Maruyama, Y. *Chem. Phys. Lett.* **1998**, *288*, 885.
(25) Lewis, G. N.; Magel, T. T.; Lipkin, D. *J. Am. Chem. Soc.* **1942**, *64*, 1774.
(26) Clark, F. T.; Drickamer, H. G. *J. Chem. Phys.* **1984**, *81*, 1024.
(27) Clark, F. T.; Drickamer, H. G. *J. Phys. Chem.* **1986**, *90*, 589.
(28) Mokhtari, A.; Fini, L.; Chesnoy, J. *J. Chem. Phys.* **1987**, *87*, 3429
(29) Engh, R. A.; Petrich, J. W.; Fleming, G. R. *J. Phys. Chem.* **1985**, *89*, 618.
(30) Stewart, J. J. P. *J. Comput. Chem.* **1989**, *10*, 209, 221.
(31) Seilmeier, A.; Kaiser, W. In *Ultrashort Laser Pulses and Applications*; Top. Appl. Phys. Vol. 60; Kaiser, W., Ed.; Springer: Berlin, 1988.
(32) Bagchi, B.; Fleming, G. R.; Oxtoby, D. W. *J. Phys. Chem.* **1983**, *78*, 7375.